

Search for $\mu^- \rightarrow e^+$ conversion: what can be learned from the SINDRUM-II positron data on a gold target

M. MacKenzie (Northwestern University), P. Murat(FNAL)

Abstract

In their 2006 paper setting the current limit on $\mu^- A \rightarrow e^- A$ conversion search on a gold target [2], the SINDRUM-II collaboration published, along with the electron momentum distribution, the momentum distribution of reconstructed positrons. Near the positron spectrum endpoint, there is a statistically significant excess of observed events over the expected background. We estimate that in the region $88 \text{ MeV}/c < p < 95 \text{ MeV}/c$ there are 13 events with an expected background of about 1-1.5 event, which has not been discussed by the authors. Those 13 events form a bump with a width consistent with the experimental resolution, making one think of a $\mu^- \rightarrow e^+$ conversion signal. However, the reconstructed position of the bump is about $1 \text{ MeV}/c$, or $\sim 4\sigma_p$, lower than the expected position of the $\mu^- \text{Au} \rightarrow e^+ \text{Ir}$ signal, which strongly discourages the exotic interpretation.

The excess, however, could be due to an exclusive dipole radiative muon capture (RMC) transition $^{197}\text{Au}(\text{GS}) \rightarrow ^{197}\text{Pt}(\text{GS})$ with the branching fraction of about $2 \cdot 10^{-4}$. Such a transition would not be resolved by the existing RMC measurements. We conclude that the exclusive RMC transitions could significantly modify the positron spectrum near the kinematic endpoint, and to fully exploit the physics potential of the upcoming experiments such as Mu2e and COMET, a better theoretical understanding of the endpoint of the RMC spectrum on nuclei is needed. A high-resolution measurement of the RMC photon spectra needs to be carried out and compared to the theoretical predictions. Without that, the sensitivity of the searches for $\mu^- A \rightarrow e^+ A$ and $\mu^- A \rightarrow e^- A$ might be severely limited by unknown probabilities of RMC transitions to the exclusive low-lying states of the daughter nuclei.

Contents

1	Introduction	2
2	Approach	3
3	Parameterization of the SINDRUM-II detector response	4
3.1	Momentum resolution	4
3.2	Tracking efficiency	5
4	RMC spectrum and k_{\max} determination	8
5	SINDRUM-II momentum scale	10
6	Events above 88 MeV and the $\mu^- A \rightarrow e^+ A$ signal	13
6.1	Positron momentum spectrum	13
6.2	Final states with a broken down daughter nucleus	14
6.3	Expected $\mu^- A \rightarrow e^+ A$ signal in the SINDRUM-II detector	15
7	An exclusive RMC transition?	18
8	Summary	19
9	Acknowledgments	20
A	Calculation of the positron energy in $\mu^- \text{Au} \rightarrow e^+ \text{Ir}$ conversion	20
	Bibliography	21

1 Introduction

The most stringent search limits on the processes of $\mu^- A \rightarrow e^+ A$ and $\mu^- A \rightarrow e^- A$ on nuclei come from the SINDRUM-II experiment :

$$Br(\mu^- \text{Ti} \rightarrow e^+ \text{Ca}) < 1.7 \cdot 10^{-12} (GS) \quad [1]$$

and

$$Br(\mu^- \text{Au} \rightarrow e^- \text{Au}) < 7 \cdot 10^{-13} \quad [2],$$

The data on the gold target have been collected in 2000, after [1] had been published, and the total total flux of stopped muons collected by SINDRUM-II on an Au target is about 1.5 times higher than the corresponding number of muon stops on Ti, $(4.37 \pm 0.32) \cdot 10^{13}$ [2] vs $(2.95 \pm 0.13) \cdot 10^{13}$ [1] muon stops respectively.

For a low background experiment, a larger number of stopped muons usually leads to a better experimental sensitivity, however, results of the search for $\mu^- A \rightarrow e^+ A$ conversion on an Au target have not been published. Nevertheless, along with the momentum spectrum of electrons, SINDRUM-II also shows the positron data [2]- see Figure 1.

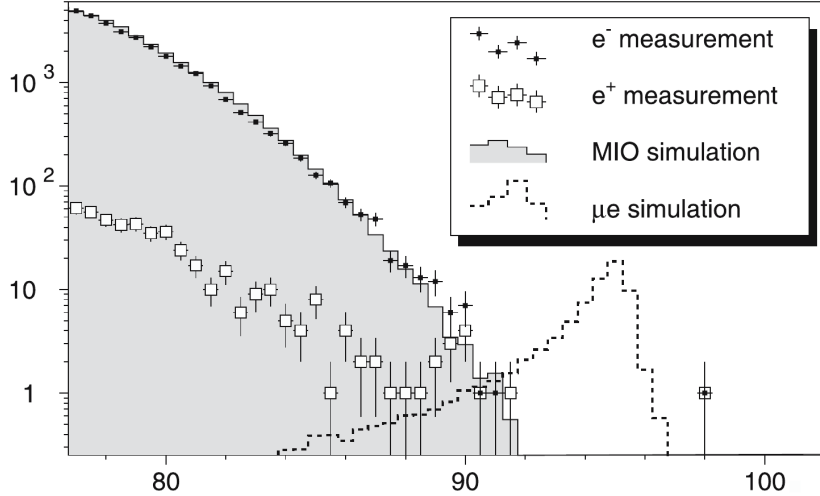


Figure 1: SINDRUM-II e^- and e^+ spectra on an ^{197}Au target from [2].

The positron momentum distribution in Figure 1 has a bump near the spectrum endpoint. This note presents an attempt to understand the origin of the bump and its implications for upcoming searches for $\mu^- A \rightarrow e^+ A$ conversion by the Mu2e and COMET experiments.

2 Approach

We start by developing a parameterized model of the SINDRUM-II detector response and tuning the model parameters to describe the electron data from [2]. The tuning procedure assumes that the measured electron spectrum is dominated by electrons produced in muon decays in orbit (DIO). This assumption doesn't take into account electrons from radiative muon capture (RMC). Those electrons are definitely present in the data, and Figure 1 shows that in the vicinity of 90 MeV/c their contribution is non-negligible and needs to be taken into account.

However, as reference [2] doesn't show the momentum spectrum of RMC electrons, which, due to the Compton scattering, is different from the RMC positron spectrum, we simply acknowledge the presence of the RMC contribution in the SINDRUM-II electron data, but don't take any action.

To model the electron data, SINDRUM-II used the DIO spectrum calculated for the muonic Pb atom, tabulated in [3]. The spectrum was corrected for the difference in the muon binding energies in muonic atoms of ^{197}Au and ^{208}Pb . The parameterized model of the SINDRUM-II detector response developed in Section 3 uses this DIO spectrum as input.

We next assume that the detector response - resolution and efficiency - is the same for electrons and positrons of the same momentum, and use the model of the SINDRUM-II detector response, tuned on electrons, to describe the positron spectrum from [2]. The spectrum is dominated by positrons coming from conversions of RMC photons in the detector material as well as from the direct production of e^+e^- pairs in the process of nuclear muon capture.

To predict the momentum spectrum of positrons, one needs to know the energy distribution of photons produced in radiative muon capture on gold. We assume that for energies at least a few MeV below the spectrum endpoint, the RMC photon spectrum can be described by the closure approximation model [4] and we fit the positron spectrum below 88 MeV/c to determine the model parameter k_{max} defining the endpoint and shape of the photon energy spectrum. After that, we predict the expected RMC contribution in the positron spectrum above 88 MeV/c and quantify the observed excess of events in that region.

Finally, we discuss if the observed excess is consistent with the signal expected from the exotic $\mu^- \text{Au} \rightarrow e^+ \text{Ir}$ transition.

3 Parameterization of the SINDRUM-II detector response

3.1 Momentum resolution

Figure 2 overlays the electron momentum spectrum measured by SINDRUM-II and the DIO spectrum on ^{208}Pb calculated in [3] and shifted by 0.5 MeV/c to account for the difference in the muon binding energies in ^{208}Pb and ^{197}Au . Both spectra are rapidly falling with momentum and have very different slopes. The sign of the difference is easy to understand: in the case of a steeply falling spectrum, the finite experimental resolution smears the spectrum and makes it less steep.

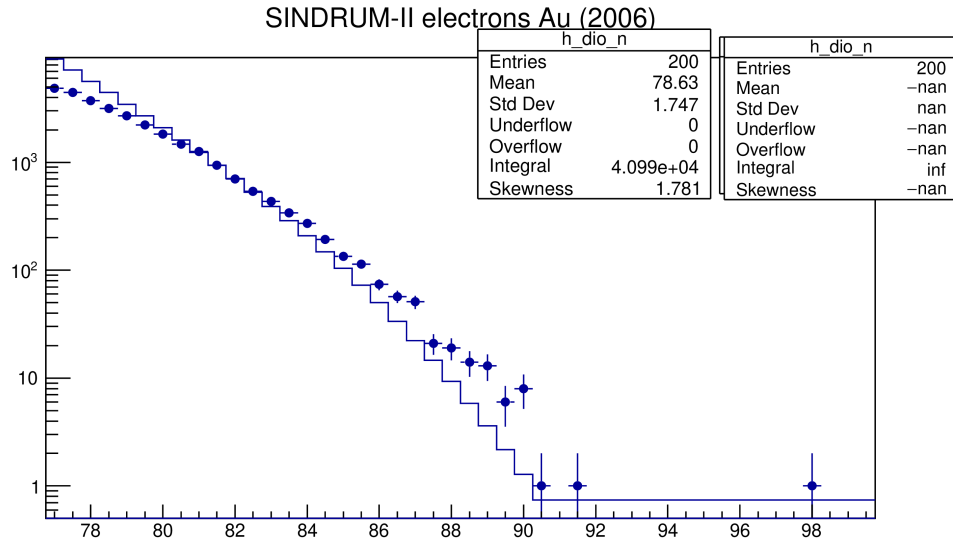


Figure 2: SINDRUM-II electron spectrum (points with the error bars) overlaid with the DIO spectrum from [3]. The theoretical spectrum, shown as a histogram, is normalized to the same area as the data for $p > 80$ MeV/c.

We make a simplifying assumption that the detector momentum response function is symmetric and can be described by a single Gaussian with a mean of 0. To choose the optimal value of the resolution parameter, σ_P , we vary its value in the range [1, 3.5] MeV/c, convolve the theoretical DIO spectrum with the res-

olution function, and use the resulting distribution to fit the SINDRUM-II electron spectrum. The fit has one parameter - the normalization. The fit χ^2 dependence on σ_P is shown in Figure ?? . The best value of the resolution parameter, $\sigma_P = 2.0 \pm 0.1$ MeV/c, is significantly higher than the SINDRUM-II momentum resolution, which is about 0.5 MeV/c. The difference is most likely due to the contribution of RMC electrons, unaccounted for in the fitting procedure. As one can see from Figure 1, for momenta close to 90 MeV/c, the RMC contribution can not be ignored. As the RMC spectrum falls less steeply than the DIO spectrum, ignoring the RMC contribution should result in a larger value of σ_P returned by the fit.

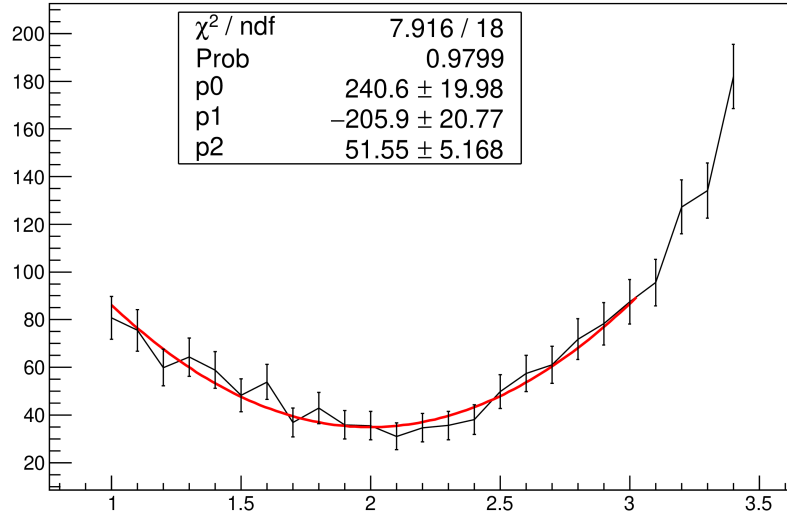


Figure 3: χ^2 of the fit of the SINDRUM-II DIO electron spectrum with the theoretical distribution convolved with a Gaussian with resolution σ_P as a function of σ_P .

3.2 Tracking efficiency

We assume that the SINDRUM-II tracking efficiency is flat for momenta $p > 80$ MeV/c. Normalizing the DIO spectrum convolved with a Gaussian resolution function with $\sigma_P = 2.0$ MeV/c to the electron data in the region $p > 80$ MeV/c, and dividing the data spectrum by the resulting distribution gives the “efficiency” dependence on the track momentum. The resulting dependence is shown in Figure

4, it is well described by a function, constant above 80 MeV/c and falling linearly below 80 MeV/c.

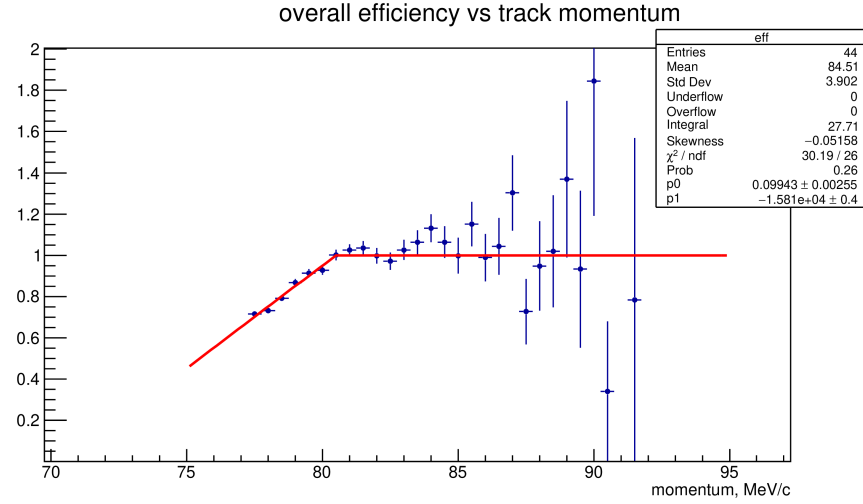


Figure 4: Parameterization of the SINDRUM-II efficiency vs the track momentum. Definition of efficiency includes all components - trigger, reconstruction, and selection. Overall normalization is chosen such that efficiency is equal to one for $p > 80$ MeV/c.

This step concludes tuning of the detector response. Figure 5 shows the description of the SINDRUM-II electron data of [2] with the tuned response - the quality of description is surprisingly good, better than one might expect from such a simplistic model.

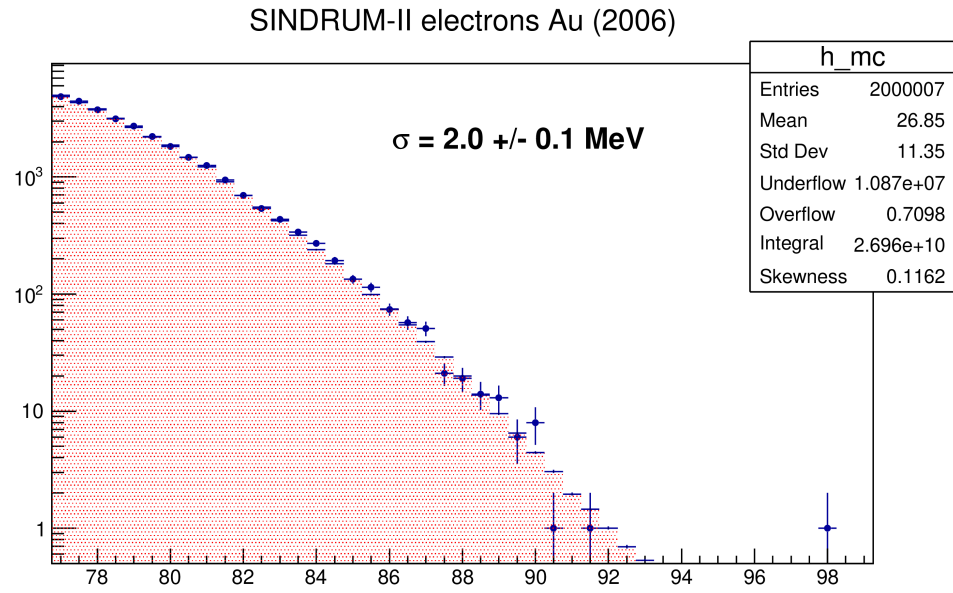


Figure 5: Description of the electron spectrum on the Au target from [2] with the tuned model of the SINDRUM-II detector response.

4 RMC spectrum and k_{\max} determination

Measured RMC photon energy spectra on nuclei can be successfully described within a closure approximation model which predicts the RMC photon spectra depending on just one parameter - the photon spectrum endpoint:

$$\frac{dN}{dE} = \frac{e^2}{\pi} \frac{k_{\max}^2}{m_\mu^2} (1 - \alpha)(1 - x + 2x^2)x(1 - x)^2$$

where E is the photon energy, k_{\max} is the energy spectrum endpoint, $\alpha = (N - Z)/A$, and $x = E/k_{\max}$ [4]. Values of k_{\max} for different nuclei are not predicted, but determined from fits to the experimental data. Typically, fits return k_{\max} values significantly, 5-15 MeV/c, lower than the kinematically allowed limits.

Internal conversions, or off-shell RMC photons, also contribute to the measured spectrum. Assuming that the energy distribution of off-shell photons is the same as the energy distribution of the on-shell photons, and the energy sharing between the positron and electron is similar in both cases, the contribution of the off-shell photons should be accounted for by the overall spectrum normalization.

We determine the value of the k_{\max} parameter by fitting the SINDRUM-II positron spectrum with a closure approximation spectrum convolved with the resolution ($\sigma_P = 2$ MeV/c) and the efficiency determined from the fit to the electron spectrum (see Figure 4) for a range of k_{\max} values. Figure 6 shows the dependence of the fit χ^2 on k_{\max} , the best fit corresponds to $k_{\max} = 88.0 \pm 0.6$ MeV. With the positron energy losses taken into account (see Section 5), the value becomes $k_{\max} = 88.6 \pm 0.6$ MeV. Consistent with the available experimental data, the maximal photon energy allowed kinematically in a $\mu^- + {}^{197}\text{Au}(\text{GS}) \rightarrow \nu + \gamma + {}^{197}\text{Pt}(\text{GS})$ transition is $E_{\max} = 94.3$ MeV, about 5 MeV higher than the k_{\max} value corresponding to the best fit.

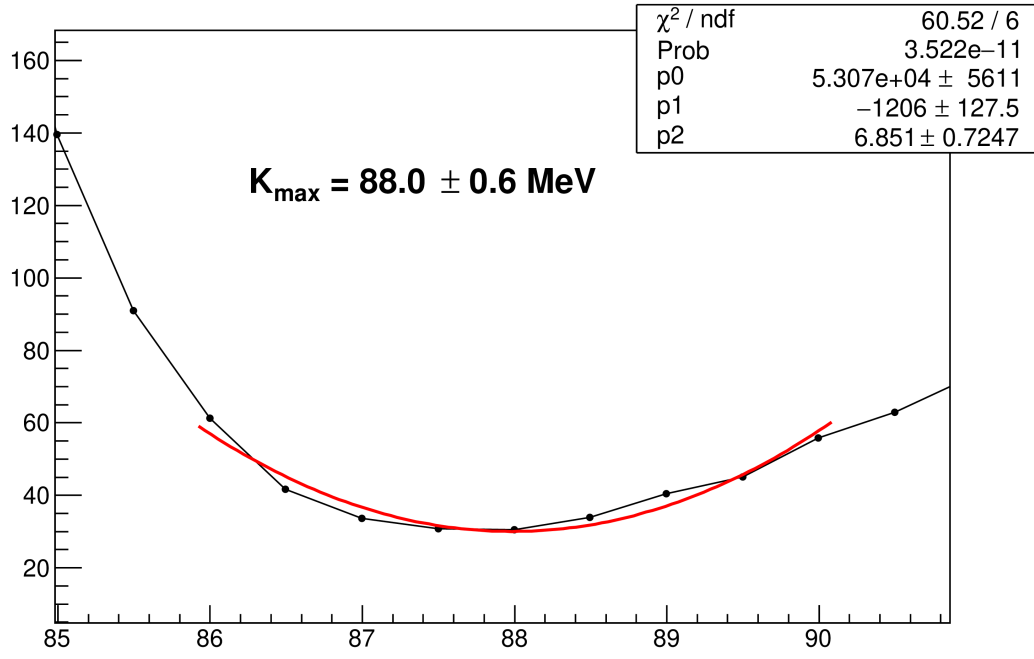


Figure 6: χ^2 of the SINDRUM-II positron spectrum fit with the positron momentum distribution derived from the RMC closure approximation spectrum convolved with the detector response as a function of k_{max} . Used in the fit are events with $p < 88 \text{ MeV}/c$.

5 SINDRUM-II momentum scale

In [2], the experimental momentum scale has been calibrated using the edge of the Michel spectrum from muon decays $\mu^+ \rightarrow e^+ \nu \bar{\nu}$ at rest. The calibration was performed with the magnetic field reduced to about 50% of the nominal value. The reconstructed positron momentum distribution is shown in Figure 7.

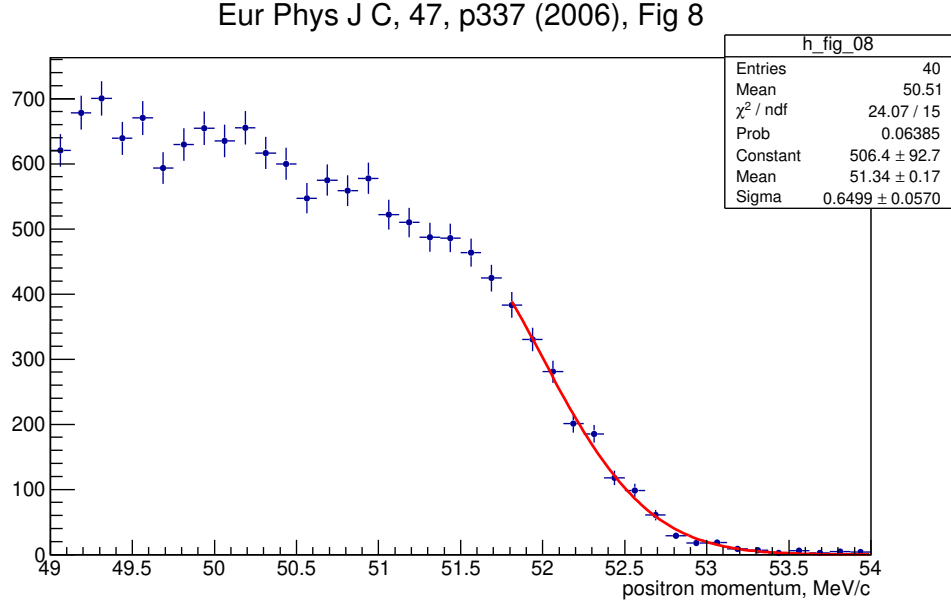


Figure 7: Reconstructed momentum spectrum of positrons from $\mu^+ \rightarrow e^+ \nu \bar{\nu}$ decays used in [2] for detector momentum calibration.

Although radiative corrections modify the positron spectrum, their impact on the edge of the Michel spectrum is fairly small, as shown in Figure 8. Therefore, the reconstructed position and shape of the edge depend primarily on the energy losses in the detector and the experimental momentum resolution.

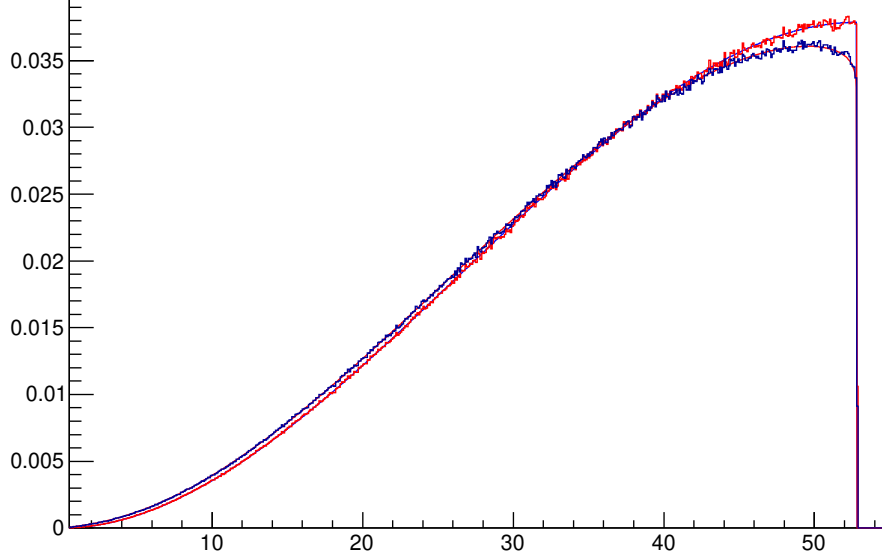


Figure 8: Theoretical Momentum spectrum of positrons from the $\mu^+ \rightarrow e^+ \nu \bar{\nu}$ decay. Red: leading order, blue: with radiative corrections taken into account.

We expect the positron momentum referred to in the paper to be the momentum in the first reconstructed point on the trajectory. As such, the reconstructed Michel edge should be affected by the energy losses in front of the tracker, as well as the tracker momentum resolution. According to [2], the energy losses in front of the tracker are due to losses in the Au target (75 mg/cm^2) and the wall of the vacuum chamber (324 mg/cm^2), most of which is aluminum and carbon fiber.

To validate our understanding of the SINDRUM-II momentum calibration, we simulate energy losses of positrons with initial momenta distributed uniformly in the range $[45, 52.8] \text{ MeV/c}$ in a structure consisting of the two layers described above. The initial momentum distribution is shown in Figure 9 in red, and the positron momentum distribution on exit from the vacuum chamber wall is shown in blue. Comparing the two distributions shows that for a 50 MeV positron, the most probable energy loss in front of the SINDRUM-II tracking chamber is about 0.6 MeV.

Shaded in Figure 9 is the positron momentum distribution which includes the energy losses in the target and the vacuum chamber wall, and is convolved with a Gaussian with $\sigma = 0.55 \text{ MeV/c}$. The value of $\sigma = 0.55 \text{ MeV/c}$ corresponds to

Simulated SINDRUM-II Michel edge calibration

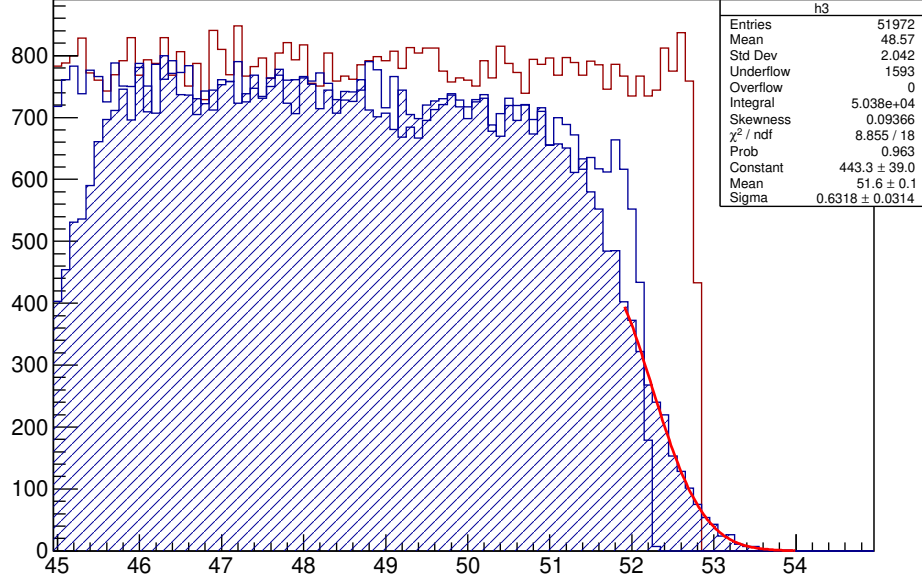


Figure 9: A flat spectrum with the right edge at 52.8 MeV is shown in red, the same spectrum convolved with the expected SINDRUM-II energy losses is in blue, and then this distribution convolved with a Gaussian with $\sigma = 0.55$ MeV/c is shaded.

the SINDRUM-II momentum resolution of 1.3 MeV/c FWHM [5]. The shaded distribution in Figure 9 double counts the fluctuations of energy losses, however the impact of double counting is small, and the momentum edge smearing is dominated by the momentum resolution of the tracker.

The fit of the high-momentum part of the smeared edge with a Gaussian returns $\sigma = 0.63 \pm 0.03$ MeV/c, in good agreement with $\sigma = 0.65 \pm 0.06$ MeV/c returned by the fit of the SINDRUM-II spectrum in Figure 7.

6 Events above 88 MeV and the $\mu^-A \rightarrow e^+A$ signal

6.1 Positron momentum spectrum

Figure 10 overlays the SINDRUM-II positron spectrum on the ^{197}Au target with the closure approximation spectrum convolved with the parameterized model of the SINDRUM-II detector response.

There are 14 events above 88 MeV/c in the data. Looking at the data above 94 MeV/c, we can estimate the background due to radiative pion capture (RPC) and cosmics to be of the order of one event. The closure approximation-based RMC model predicts about 0.4 events above 88 MeV/c.

One therefore needs to ask whether the closure approximation reliably describes the RMC positron spectrum near the endpoint. In particular, the closure approximation doesn't take into account RMC transitions to the exclusive low-lying states of the daughter nucleus.

In the case of the ^{197}Au target, a dipole transition $^{197}\text{Au} \rightarrow ^{197}\text{Pt}$ to the ground state of the Pt nucleus is allowed. Given that the energy splitting between an electron and a positron from a photon conversion is almost uniform, the positron spectrum corresponding to such a transition, in a first order approximation, should be flat. Taking into account the energy losses, the positron momentum spectrum could extend up to 93.2 MeV/c. Therefore, if it existed, such a transition could reduce the tension between the background model and the data. Below, we estimate the probability of such a transition corresponding to 13 RMC events in the region $88 \text{ MeV/c} < p_{e^+} < 93.2 \text{ MeV/c}$.

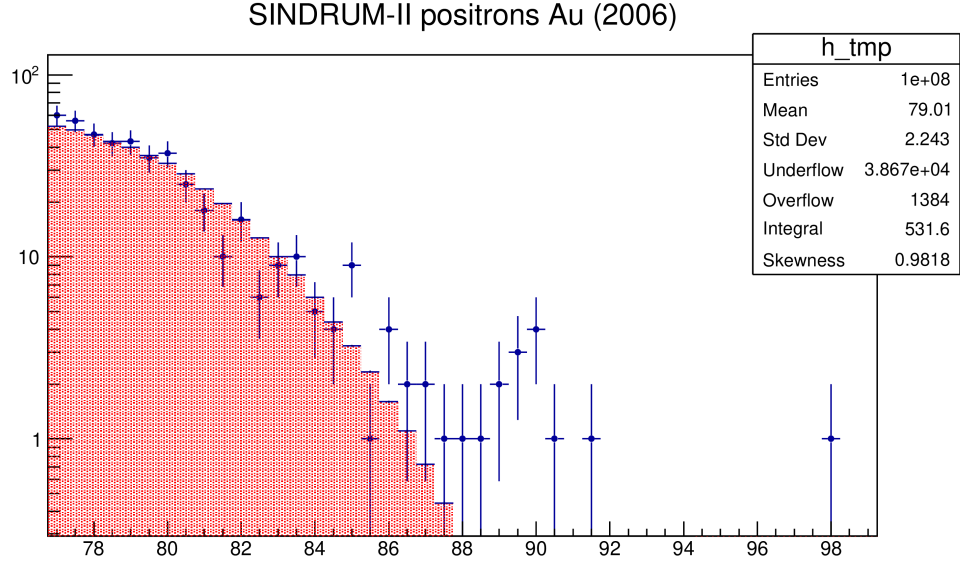


Figure 10: Fit of the SINDRUM-II positron spectrum with the closure approximation spectrum convolved with the parameterized model of the SINDRUM-II detector response. The closure approximation parameter $k_{max} = 88$ MeV/c.

6.2 Final states with a broken down daughter nucleus

As a daughter nucleus produced in the process of radiative muon capture can break down and emit one or several protons or neutrons, one could also ask whether photons from transitions of

$$\mu + {}^{197}\text{Au} \rightarrow \gamma + \nu + {}^{197-k}\text{Pt} + k \text{ neutrons}$$

or

$$\mu + {}^{197}\text{Au} \rightarrow \gamma + \nu + {}^{197-k}A_{Z=78-k} + k \text{ protons}$$

could produce positrons with a higher energy spectrum endpoint than the $\mu + {}^{197}\text{Au} \rightarrow \gamma + \nu + {}^{197}\text{Pt}$ transition. Figure 11 shows the distributions of mass differences between the final states consisting of (${}^{197-k}\text{Pt} + k$ neutrons) and (${}^{197-k}A_{Z=78-k} + k$ protons), and the ground state of the ${}^{197}\text{Pt}$ nucleus. Based on those distributions one can conclude that events with the most energetic photons and, as such, most energetic positrons, should correspond to transitions with the ${}^{197}\text{Pt}$ nucleus in the final state, with a reconstructed positron momentum endpoint of 93.2 MeV/c. As the positron momentum spectrum extends up to about 92

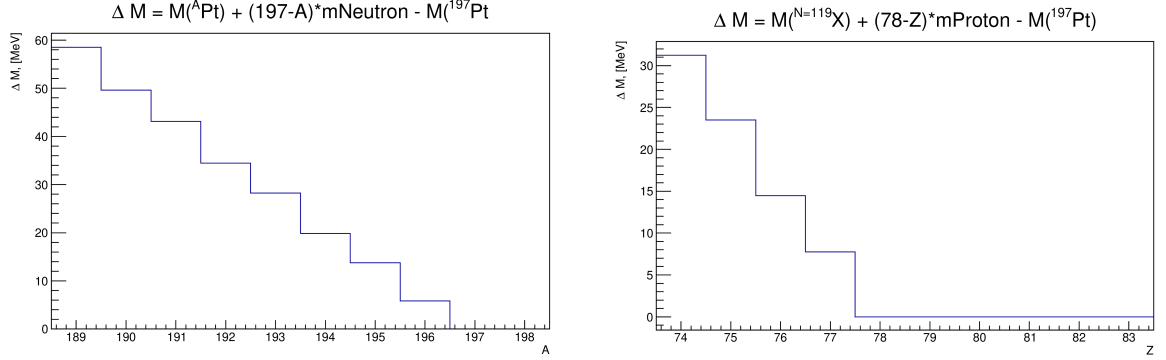


Figure 11: Mass differences between the final state with the broken down daughter nucleus and ^{197}Pt for different breakdown scenarios of ^{197}Pt nucleus. Isotope masses taken from [6]. The final state with the ^{197}Pt nucleus always has the lowest mass and, therefore, the highest photon spectrum endpoint.

MeV/c, final states with masses higher than the mass of the ^{197}Pt ground state by $\sim 1.2 \text{ MeV}/c^2$ couldn't contribute to the excess.

6.3 Expected $\mu^- \text{A} \rightarrow e^+ \text{A}$ signal in the SINDRUM-II detector

One could ask whether the excess of events on the high-momentum tail of the positron momentum distribution is consistent with the signal expected from $\mu^- \rightarrow e^+$ conversion on gold. Figure 12 shows the expected $\mu^- \rightarrow e^-$ signal in the SINDRUM-II detector, digitized from Figure 11 of [2]. The conversion peak has its maximum at 95.0 MeV/c, consistent with the most probable energy losses of 0.6 MeV in front of the tracker, discussed in Section 5. The expected position of the $\mu^- \text{Au} \rightarrow e^+ \text{Ir}$ conversion signal is about 3.9 MeV/c lower than for the $\mu^- \text{Au} \rightarrow e^- \text{Au}$ signal; the difference is small enough to not affect the momentum resolution.

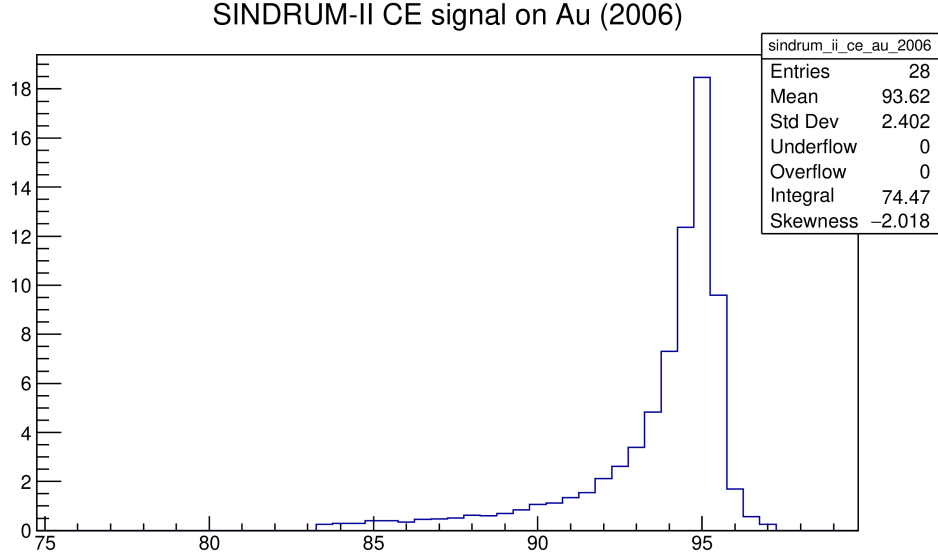


Figure 12: The expected position and shape of the $\mu^- \rightarrow e^-$ conversion signal on Au in the SINDRUM-II detector.

We therefore assume that the expected position and the shape of the positron signal from $\mu^- \rightarrow e^+$ conversion reconstructed in the SINDRUM-II detector can be reproduced by moving the $\mu^- \rightarrow e^-$ signal shown in Figure 12 down by 4 MeV/c. The expected $\mu^- A \rightarrow e^+ A$ signal is shown in Figure 13 together with the SINDRUM-II positron data and the RMC background. The RMC normalization comes from the fit in the region $p < 88$ MeV/c, explained in Section 4. To guide the eye, the $\mu^- \rightarrow e^+$ conversion signal is normalized to 20 events.

The excess of events above 88 MeV/c has a shape consistent with the shape of the expected $\mu^- \rightarrow e^+$ signal; however, the average momentum of the data events in the group is about 1 MeV/c lower than expected from the signal. The estimated statistical uncertainty on the position of the center of gravity of those events is 0.24 MeV/c, so the expected position of the $\mu^- \rightarrow e^+$ conversion signal is about 4σ higher than calculated from the data. An attempt to fit the data in the range [89, 92] MeV/c with the function having the shape of the $\mu^- \rightarrow e^+$ conversion signal returns a p-value of 0.004. This strongly disfavors the exotic (μe conversion) interpretation of the excess.

The track charge mis-identification probability in the SINDRUM-II detector is about 0.2% [1], which can't explain the excess of positron events.

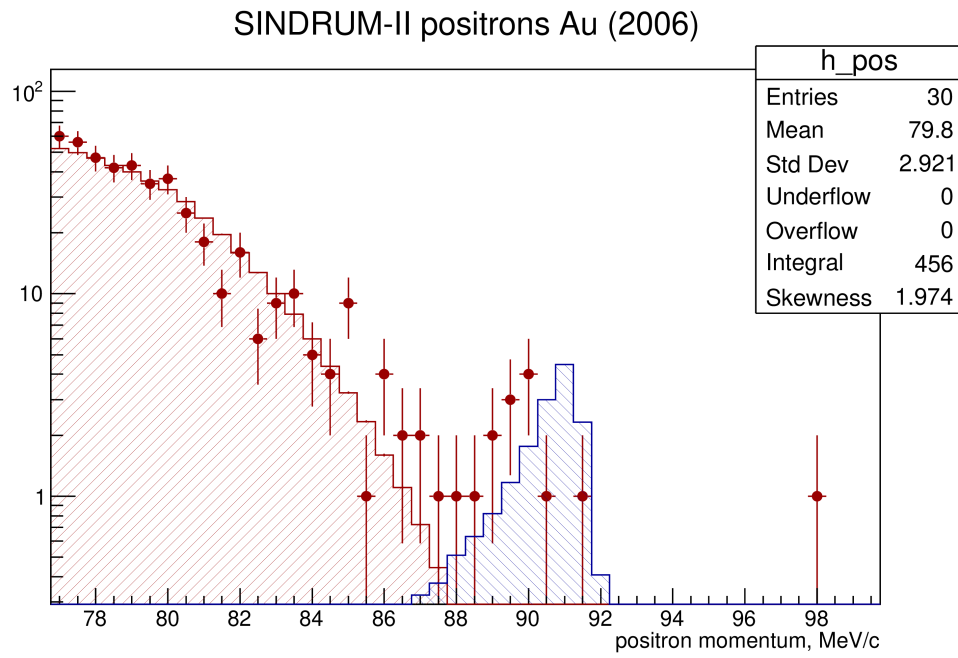


Figure 13: SINDRUM-II positron spectrum overlaid with the expected background from RMC and a signal from $\mu^- \text{Au} \rightarrow e^+ \text{Ir}$ normalized to 20 events. Normalization of the signal is chosen to guide the eye.

7 An exclusive RMC transition?

As it has already been mentioned, the excess of the positron events in the tail could be explained by the contribution of RMC accompanied by a nuclear transition from the ground state of ^{197}Au to an exclusive final state of ^{197}Pt . As the ground state of ^{197}Au has spin parity $3/2^+$ and the ground state of ^{197}Pt has spin-parity of $1/2^-$, an allowed dipole transition between the two states could result in mono-energetic photons with the energy $E = 94.3 \text{ MeV}$. A uniform, in a first order approximation, distribution of the electron-positron energy splitting could result in a flat contribution extending up to $p = 93.2 \text{ MeV}/c$ added to the rapidly falling measured positron spectrum from converted RMC photons.

In total, the SINDRUM-II positron spectrum on a gold target has 456 events with $p > 77 \text{ MeV}/c$. 14 out of 456 events have $p > 88 \text{ MeV}/c$. Attributing one event - with the highest momentum - to cosmics/RPC, there are 13 events left with reconstructed positron momenta in the region 88-93 MeV/c. Assuming that all of them are due to an $\text{Au}(\text{GS}) \rightarrow \text{Pt}(\text{GS})$ RMC transition and a flat positron spectrum from 0 - 93 MeV/c, we estimate the total number of such events as $13 \text{ events}/5 \text{ MeV}/c \cdot 93 \text{ MeV}/c \approx 250 \text{ events}$.

For an RMC spectrum with $k_{\text{max}} = 88 \text{ MeV}$, shown in Figure 14, about 14% of photons have energies above 57 MeV. The TRIUMF RMC spectrometer measured 2000-3000 data events per target [7]. For an experimental energy cutoff $E > 57 \text{ MeV}$, that translates into 15,000 - 20,000 events in the whole spectrum.

Similarly, for $k_{\text{max}} = 88 \text{ MeV}$, about $3.3 \cdot 10^{-4}$ of all RMC positrons have $p > 77 \text{ MeV}/c$. Assuming a momentum-independent efficiency, 442 reconstructed events with $p > 77 \text{ MeV}/c$ corresponds to $1.3 \cdot 10^6$ RMC events in the full spectrum and $1.9 \cdot 10^5$ RMC events with photon energies above 57 MeV. This is two orders of magnitude higher than the per-target statistics of the TRIUMF RMC spectrometer.

The branching ratio of the exclusive transition could be estimated at $\sim 2.5 \cdot 10^2 / 1.3 \cdot 10^6 \sim 2 \cdot 10^{-4}$, so for typical per-target statistics of [7], one would expect such a transition to contribute $2 \cdot 10^4 \cdot 2 \cdot 10^{-4} \sim 5$ events. Given the photon energy resolution of $\text{FWHM} \sim 7 \text{ MeV}$, it would be rather difficult for the TRIUMF RMC spectrometer to resolve transitions of that strength in the measured spectra. However, a measurement with a photon energy resolution of about 1 MeV and statistics an order of magnitude higher than that of [7] would allow one to see such a transition.

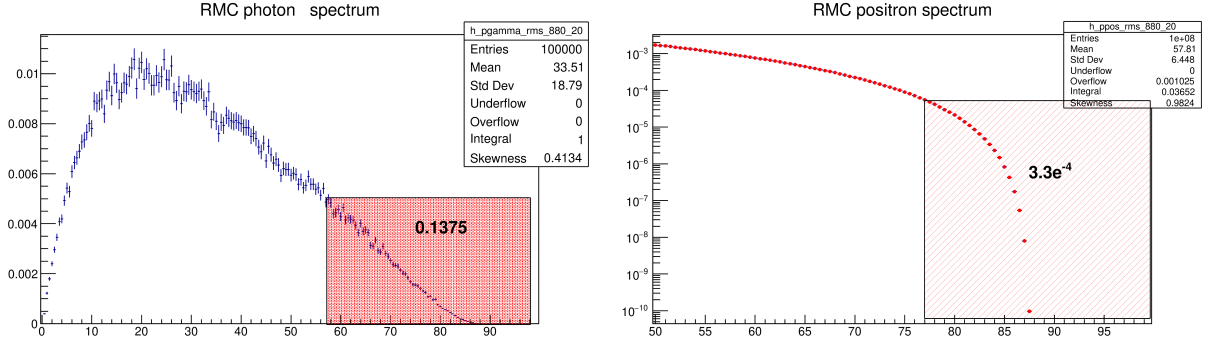


Figure 14: RMC photon (left) and e^+ (right) momentum spectra, $k_{\max} = 88$ MeV.

8 Summary

In their 2006 paper which sets the current best limit on $\mu^- A \rightarrow e^- A$ on a gold target [2], the SINDRUM-II collaboration published, along with the electron momentum distribution, the momentum distribution of reconstructed positrons. Near the positron spectrum endpoint, there is an excess of events which has not been discussed by the authors.

To understand the origin and potential implications of this excess, we developed a simple detector response model, tuned it using the SINDRUM-II electron data, and used the tuned model to describe the positron data. The excess of high-momentum events in the positron data is statistically significant, comprised of about 13 events with the background expectation of about 1.4. The background expectation is dominantly due to RPC and cosmics, the RMC background above 88 MeV/c is < 1 event.

Interestingly, the excess has a width consistent with the SINDRUM-II detector resolution. The expected position of the $\mu^- \text{Au} \rightarrow e^+ \text{Ir}$ signal is 1 MeV/c, or $\sim 4\sigma_p$, higher, and fitting those events with the $\mu^- \rightarrow e^+$ signal shape has a p-value of 0.004; this strongly discourages the exotic interpretation.

The excess could be due to an exclusive dipole RMC transition between $^{197}\text{Au}(\text{GS}) \rightarrow ^{197}\text{Pt}(\text{GS})$, with a branching fraction of about $2 \cdot 10^{-4}$. Given the statistics and resolution of the published RMC measurements, such a transition would not be resolved experimentally.

The observation has significant implications for the upcoming searches for processes of $\mu^- A \rightarrow e^+ A$ and $\mu^- A \rightarrow e^- A$ conversion. In the $\mu^- A \rightarrow e^+ A$ channel, exclusive RMC transitions could simply fake the signal; in the $\mu^- A \rightarrow e^- A$

channel, those transitions could significantly distort the predicted SM background shape.

To fully exploit the physics potential of experiments such as Mu2e and COMET, a better theoretical understanding of the endpoint of the RMC spectrum on nuclei is needed. A high-resolution measurement of the RMC photon spectra needs to be carried out and compared to the theoretical predictions. Without that, the sensitivity of the upcoming searches might be limited by the unknown probabilities of RMC transitions to the exclusive low lying states of the daughter nuclei.

9 Acknowledgments

We want to thank our colleagues at Mu2e, who offered advice for this study. We also appreciate the Velasco group at Northwestern for encouraging M. MacKenzie to participate in these studies. His research was in part funded by the “Research in the Energy, Cosmic and Intensity Frontiers at Northwestern University” award, DE-SC0015910. Work of P.Murat was supported by the Fermi National Accelerator Laboratory, managed and operated by Fermi Research Alliance, LLC under Contract No. DE-AC02-07CH11359 with the U.S. Department of Energy. The U.S. Government retains and the publisher, by accepting the article for publication, acknowledges that the U.S. Government retains a non-exclusive, paid-up, irrevocable, world-wide license to publish or reproduce the published form of this manuscript, or allow others to do so, for U.S. Government purposes.

A Calculation of the positron energy in $\mu^- \text{Au} \rightarrow e^+ \text{Ir}$ conversion

We consider only the ground state conversion process. For this, the conversion energy is given by:

$$E_{e^+} = m_\mu - B_\mu - E_{recoil} - \Delta_{Z-2}$$

where m_μ is the muon mass, B_μ is the binding energy of the 1s energy level, E_{recoil} is the kinetic energy of the recoiling nucleus, and Δ_{Z-2} is the difference between the incoming and outgoing nuclear masses.

Since the muon orbit is ~ 200 times closer to the nucleus than the electrons’, one can assume the electrons do not contribute to the muon capture process.

Parameter	Value
m_μ	105.6583745(24) MeV/c ² [8]
m_e	0.5109989461(31) MeV/c ² [8]
$1u$	931.49410242(28) MeV/c ² [8]
B_μ	10081.23 keV [9]
$A_r(^{197}\text{Au})$	196.96656879(71) u [6]
$M_N(^{197}\text{Au})$	183432.828(1) MeV/c ²
$A_r(^{197}\text{Ir})$	196.969 655(22) u [6]
$M_N(^{197}\text{Ir})$	183436.725(21) MeV/c ²
Δ_{Z-2}	3.897(21) MeV/c ²

Table 1: Parameters used in the $\mu^- \text{Au} \rightarrow e^+ \text{Ir}$ positron energy calculation.

Therefore, the electron masses are not considered and instead only the nuclear masses are used: $M_N = M_A - Z \cdot m_e$, where $M_A = A_r \cdot u$, A_r is the relative mass, u is the atomic mass unit, and m_e is the electron mass.

The recoiling energy is given by considering the two body decay: $N(\mu^- + ^{197}\text{Au}) \rightarrow e^+ + ^{197}\text{Ir}$. Considering the rest frame of the muonic gold atom, the decay products must satisfy $p_{e^+} + p_{^{197}\text{Ir}} = p_o = 0$. The energy of the iridium nucleus is then given by:

$$E_{^{197}\text{Ir}} = \frac{M^2 + M_N(^{197}\text{Ir})^2 - m_e^2}{2M} = E_{recoil} + M_N(^{197}\text{Ir})$$

where M is the mass of the muonic gold nucleus system, $M = M_N(^{197}\text{Au}) + m_\mu - B_\mu = 183528.405 \text{ MeV/c}^2$. Using the parameters in Table 1, we get $E_{recoil} = 0.023 \text{ MeV}$.

Combining these together, the $\mu^- \text{Au} \rightarrow e^+ \text{Ir}$ positron energy for the ground state transition is $E_{e^+} = 91.657(21) \text{ MeV}$, where the uncertainty on B_μ is assumed to be $\sim 1 \text{ keV}$.

References

- [1] Kaulard, J. and others (SINDRUM II), Phys. Lett. B, **422**, 334 (1998)
- [2] W. H. Bertl et al. (SINDRUM II), Eur. Phys. J. C **47**, 337 (2006).

- [3] R. Watanabe, K. Muto, T. Oda, T. Niwa, H. Ohtsubo, R. Morita, and M. Morita, Atomic Data and Nuclear Data Tables, **54**, 1, 165 (1993)
- [4] H.P.C. Rood and H.A. Tolhoek, Nuclear Physics, **70**, 3, 658 (1965)
- [5] Kaulard, Joerg, PhD Thesis, RWTH, Aachen, unpublished, in German (1997)
- [6] G. Audi, F.G. Kondev, Meng Wang, W.J. Huangand, and S. Naimi, The NUBASE 2016 evaluation of nuclear properties, Chinese Physics C, v41, 030001 (2017)
- [7] Bergbusch, P.C. et al, Phys. Rev. C, **59**, 2853 (1999)
- [8] P.A. Zyla et al. (Particle Data Group), Prog. Theor. Exp. Phys. **2020**, 083C01 (2020).
- [9] R.Engfer, H.Schneuwly, J.L.Vuilleumier, H.K.Walter and A.Zehnder, ATOMIC DATA AND NUCLEAR DATA TABLES **14**, 509 (1974)